PERGAMON

International Journal of Solids and Structures 38 (2001) 2009–2023

INTERNATIONAL JOURNAL OF SOLIDS and STRUCTURES

www.elsevier.com/locate/ijsolstr

Pre-shaping motion input for a rotating flexible link

Giovanni Mimmi [a,*], Paolo Pennacchi [b,1]

[a] *Dipartimento di Meccanica Strutturale, Università degli studi di Pavia, Via Ferrata, 1, I-27100 Pavia, Italy*
[b] *Dipartimento di Meccanica, Politecnico di Milano, P.zza L. da Vinci, 32, I-20133 Milano, Italy*

Received 10 July 1999; in revised form 13 January 2000

Abstract

The interest in the design of manipulators for space operations with a light structure has grown meaningfully in comparison with rigid manipulators, even if these flexible manipulators are unavoidably characterized by a nonnegligible structural flexibility. This paper deals with the first phase of a project financed by a grant from the Italian Space Agency, which is concerned with the setting up of an open-loop control for a planar manipulator with flexible linkages. In this phase, the project is subdivided into two parts: on the one hand, different command inputs have been proposed for point-to-point operations; on the other hand, dynamic simulations have been carried out by using a multibody model with flexible parts, in order to evaluate the residual vibrations due to the selected command input at the end of the motion. These command inputs will be applied to the actual manipulator, which is already available, in a future phase of the project. The command inputs, which are described here, are based on both the convolution of special impulse inputs suitably chosen on the basis of the system natural frequencies and the reduction of impulsive inertia forces by means of a suitable algorithm proposed here and derived from cam design. The simulations are carried out by commercial software for the study of multibody systems and custom programs for the command input implementation. The results obtained for the residual vibrations are compared to those obtained by conventional command inputs in the simulations on the same model.

Keywords: Flexible manipulators; Open-loop control; Input motion pre-shaping

1. Introduction

The present paper describes a part of a larger project concerning the analysis of the control of a manipulator with a couple of flexible links for spatial duties. Due to the aims of the present paper, which deals with the comparison of different motion inputs on the basis of the residual vibration at the end of the positioning, here we are taking into consideration an arm constituted by a single link only, and we have considered all the other parts of the structure as being still. This has been done in order to have a better

* Corresponding author. Tel.: +39-0382-505-452; fax: +39-0382-528-422.
E-mail addresses: mimmi@unipv.it (G. Mimmi), paolo.pennacchi@mecc.polimi.it (P. Pennacchi).
[1] Tel.: +39-02-2399-4783; fax: +39-02-7063-8377.

0020-7683/01/$ - see front matter
PII: S0020-7683(00)00149-9

evaluation of the results and to avoid introducing undesirable torsional components due to the presence of several bodies linked by revolute joints. This latter problem could arise if all the parts of the manipulator were moved simultaneously.

In particular, the authors have considered the open-loop control of the manipulator (Mimmi et al., 1999) by operating on two levels. On the one hand, the analytical model of the manipulator has been setup and various command inputs have been tested on this model by means of numerical simulations. On the other hand, since an experimental setup was available, the same motion inputs have been applied to the manipulator and the results, as regards the reduction of the residual vibration, compared. The choice of an open-loop control has been done in view of the use of the structure in space. Therefore, the use of sensors and feed-back control devices should be avoided due to the necessity of reducing payloads. The description of the model used for the simulation and the results obtained are the main topic of this paper. First of all, the motion inputs employed are described, and a brief theoretical support is also given; then, the system is characterized by identifying the lateral modes in the operating plane. Finally, the mathematical model obtained is presented and the results compared, by means of simulation, in order to verify the possibility of reducing residual vibrations at the end of the positioning.

2. Motion inputs

An open-loop control can be adopted, by considering the particular use of the manipulator. In fact both the manoeuvres and the loading conditions during operation can be forecasted a priori. Moreover, the use of the open-loop control reduces the energy requirements to the minimum level required for the positioning. On the contrary, a closed-loop control usually also requires energy for corrections. These results appear particularly relevant for use in space.

The problem of the open-loop control of flexible structures has been considered by many authors. The motion input that gives the minimum positioning time with null residual vibrations, following the optimal control theory, is the ''bang-bang'' motion input, made up of a sequence of steps of alternate sign (Meckl and Seering, 1985a). However, if the sign inversion instants do not correspond with extreme precision to those required by the theory, relevant residual vibrations may remain. Meckl and Seering (1985a, b) deal with the problem of positioning of a robotic arm with lumped parameters. As an alternative to the ''bang-bang'' input, they suggest the control by means of a ''ramped sinusoid'' motion input that gives a slightly higher positioning time, but with fewer possibilities of exciting the natural modes of the system. Onsai and Akay (1991) analyze the implementation of a ''bang-bang'' control on a flexible arm by considering both the problem of realizing an actuator able to give the required stepping behavior for the motion torque and the problem of the uncontrolled modes. Jayasuriya and Choura (1991) consider the problem of the open-loop control of a flexible arm and give an alternative solution to both the ''bang-bang'' and the ''ramped sinusoids''. Bhat and Miu (1990) analyze a similar case by operating in both the time and frequency domains.

Different types of motion inputs, based on different design principles, have been discussed in this paper. Two basic types of inputs are considered: the first motion input which is considered, mainly to have a benchmark for the following results, is a constant acceleration input that represents the simplest motion input. The performances obtained are not as good as foreseen, due to the presence of the impulsive variation of the acceleration that excites several natural modes of the structure. In order to avoid this, a motion input based on a modified trapezoid path for the acceleration has been adopted, as is usually done in motion input for automatic machines. The theory of the pre-shaping has been applied to both the previous motion inputs. In order to do this, the first natural lateral frequency of the system has been identified.

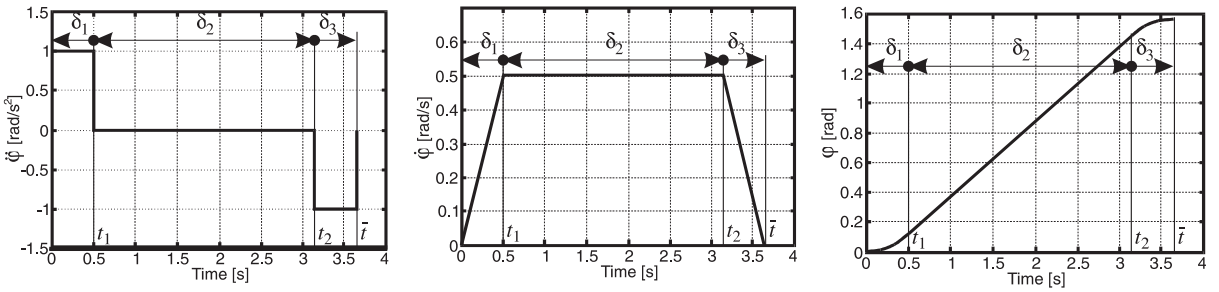

Fig. 1. Constant acceleration motion input.

2.1. Constant acceleration motion input

This is also defined as *double step motion input*, due to the shape of the acceleration profile. A null acceleration segment (and maximum velocity) follows a first segment with constant acceleration, while another segment with constant acceleration of the opposite sign ends the sequence (Fig. 1). Once the rotation $\bar{\varphi}$ to be performed is established and the maximum speed $\dot{\varphi}_{\max}$ and acceleration $\ddot{\varphi}_{\max}$ are imposed, it is possible to calculate the duration $\bar{t}$ of the operation and the values t_1 and t_2, which correspond to the shift from positive to null acceleration and from null to negative, respectively. The details of the calculation are reported in Appendix A.

2.2. Modified trapezoid motion input

The problem of the reduction of the impulsive variation of the inertia forces usually occurs in the design of mechanisms for "alternate" motion. The algorithm proposed here is based on this principle. In order to obtain this result, motion input based on a modified trapezoid is very effective, in which the initial ramp is formed by a sinusoid arc. As compared to the original algorithm for the input generation, proposed by Magnani and Ruggieri (1986), which considers time and rotation as being independent of each other, the algorithm proposed here determines the minimum possible time $\bar{t}$ for the rotation on the basis of the physical characteristics of the motor. In this case, the constraint is on the maximum velocity $\dot{\varphi}_{\max}$. For further details, see Appendix A.

2.3. Pre-shaping by means of pulse superimposition

The pre-shaping technique can be applied to every motion input; therefore, it is used on both the previously mentioned motion inputs. The use of a pulse sequence superimposed on the motion input has its origin in the concept that a step of a certain amplitude can be split into two smaller steps, one of which is delayed in time (Smith, 1958). By tuning the delay for a linear system with one d.o.f., the effect of superimposition causes the deletion of the vibration. This principle presents two weak points, since it is suitable for linear systems only and systems whose natural frequencies and damping are known exactly. Improvements in this field have been achieved by Singer and Seering (1990) as regards the robustness, since it is shown that, by increasing the number of pulses calibrated on the natural frequency, the control is more robust as regards the uncertainty on both the frequencies and damping. Improvements have also been

achieved by Singh and Heppler (1993) for applications on flexible structures. In the case proposed here, the first two natural frequencies and a three pulse sequence are considered.

A consequence of the application of this method is the increase of the system operating time, due to convolution with the original motion input. Two examples of pre-shaping are reported in Figs. 2 and 3, which show the constant acceleration and the modified trapezoid motion inputs, respectively. The corresponding motion inputs obtained by pre-shaping with two pulses calibrated on the first natural frequency are also reported. The increase of the operation time is comparable to the period of the frequency considered for each pulse. Further details are reported in Appendix A. It is worthwhile noting the different theoretical principles between the reduction of the residual vibration obtained by the modified trapezoid and the pre-shaped modified trapezoid motion inputs. In the first case, only the impulsive part of the acceleration is removed, and this can be done in different ways, depending on the amplitude of the steps of the sinusoidal arcs, and the fact whether some natural frequencies of the system are excited is not taken into consideration. In the second case, the approach is totally different, since the original motion input on which the pulses are superimposed is not important, because the method operates directly on the first natural frequencies of the system.

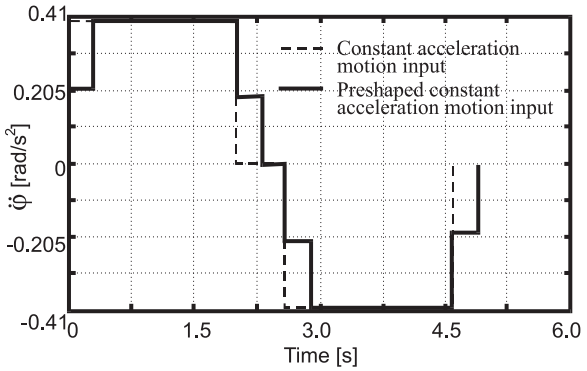

Fig. 2. Constant acceleration and pre-shaped constant acceleration motion input.

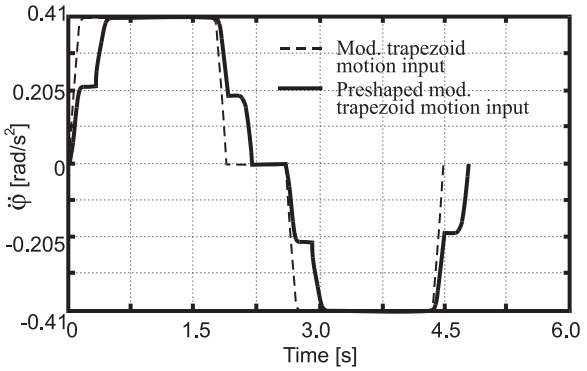

Fig. 3. Modified trapezoid and pre-shaped modified trapezoid motion input.

3. Identification of system parameters

The use of the pre-shaping method requires a knowledge of the natural frequencies and of the damping of the system with a certain precision. As the theory shows, the use of several pulses increases the robustness of the system, by accepting a 20% uncertainty on the value of the first natural frequency and of the damping. The determination of the first lateral frequencies of the system has been carried out by using three different methods.

The first one is the analytical determination of the natural frequencies by means of Euler's beam theory (Thomson, 1993; Rao, 1995); the second is the experimental determination, using an accelerometer at the free end of the forearm and two strain gauges close to the revolute joint and by exciting the structure by an impulsive force. The filtered FFT spectrum of the accelerometer signal has been reported in Fig. 4 and the results given in Eq. (1).

$$f_1 = 1.56 \text{ Hz}, \qquad f_2 = 9.72 \text{ Hz}, \qquad f_3 = 29.2 \text{ Hz}, \qquad f_4 = 50.1 \text{ Hz}. \tag{1}$$

The third method, which uses finite elements, is the only one reported in detail since it has shown good fitting both with the analytical and the experimental method and it is directly implemented into the simulation software used.

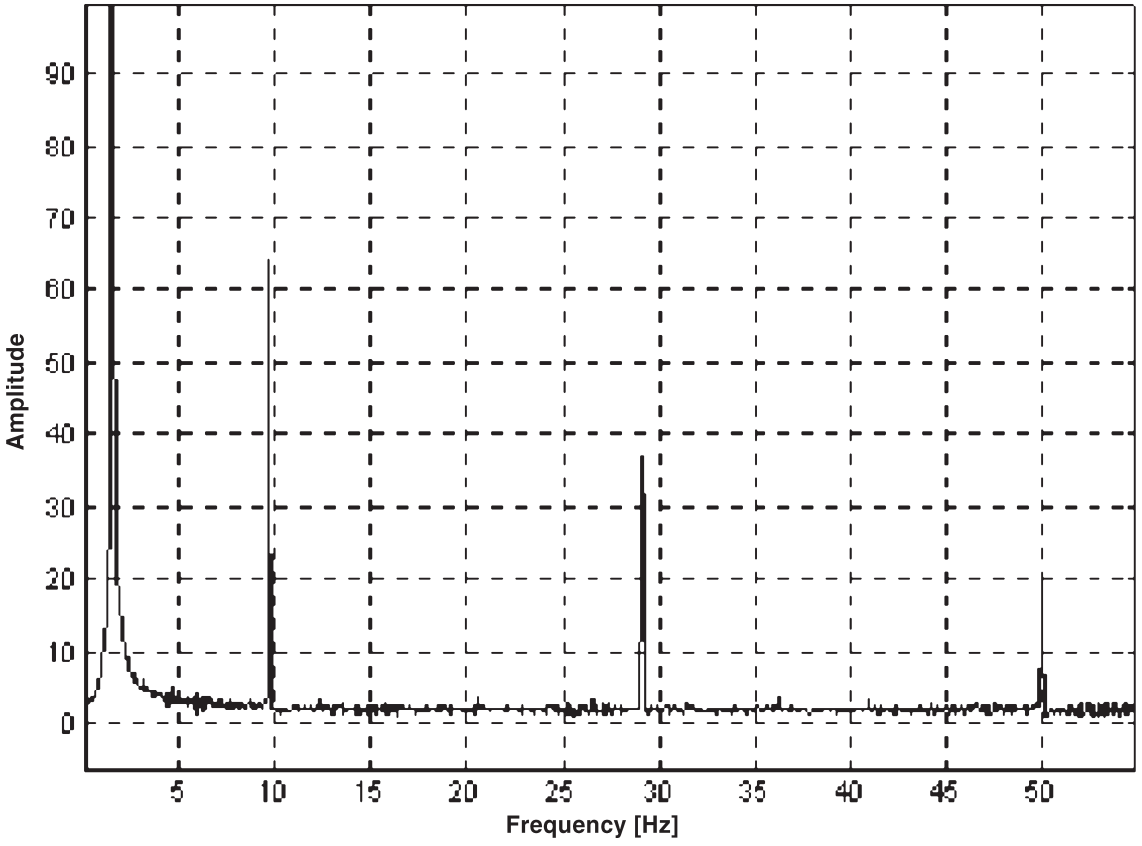

Fig. 4. FFT spectrum of forearm free-end acceleration (lateral vibration).

3.1. Determination of the natural frequencies by means of the module ADAMS/linear

Due to its simple geometry, the arm considered has been easily modeled with MSC/NASTRAN f.e.m. software, using 20 2D plate elements (Fig. 5). The model has been imported into ADAMS software and an eigenvalue analysis has been performed by the module ADAMS/*linear* that allows us to determine the first 32 modes, including the torsional and lateral modes in the plane *yz* also. In the present case, only the first four lateral modes in the plane *xy* are considered. These have the following natural frequencies (Fig. 6):

$$f_1 = 1.63 \text{ Hz}, \qquad f_2 = 10.2 \text{ Hz}, \qquad f_3 = 28.1 \text{ Hz}, \qquad f_4 = 54.69 \text{ Hz}. \tag{2}$$

The comparison of the values obtained by the three methods shows that the differences are very minimal. The most important comparison is between the experimental values and the values obtained by the analysis by ADAMS/*linear*. Since the differences are very minimal in this case, the values obtained by means of *linear* have been adopted for use during the simulations. The greatest difference is observed in the fourth

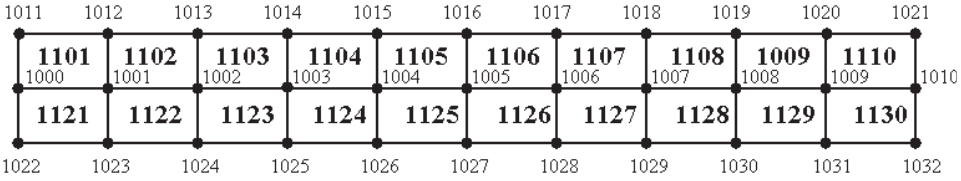

Fig. 5. Finite element mesh of the forearm.

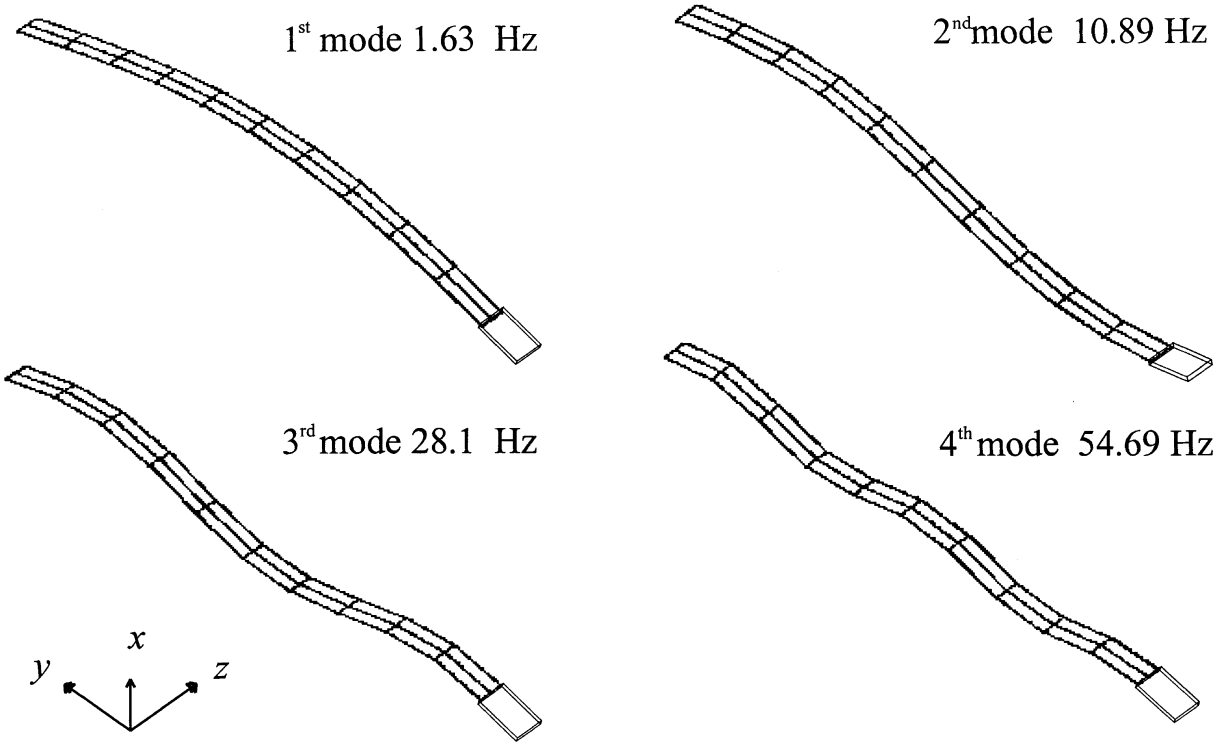

Fig. 6. Forearm lateral vibration modes.

mode, which is less important in this case, since only the first two natural frequencies are used for the pre-shaping.

3.2. Determination of the system damping

Based on several experimental tests with the impulsive force, by means of the logarithmic decay, it has been possible to determine a value of the damping ratio equal to

$$\xi = 0.0458. \tag{3}$$

4. System response simulations

The model of the manipulator arm has been implemented in ADAMS by means of the f.e.m. model described previously and of a revolute joint on which the different motion inputs have been applied. This choice requires a motor which can follow the imposed velocity and acceleration precisely in the experimental set-up and with a perfectly rigid behavior during the motion. The motion inputs implemented are in the following order:

- constant acceleration motion input;
- constant acceleration motion input, pre-shaping with one frequency and two pulses;
- constant acceleration motion input, pre-shaping with one frequency and three pulses;
- constant acceleration motion input, pre-shaping with two frequencies and three pulses;
- modified trapezoid motion input;
- modified trapezoid motion input, pre-shaping with one frequency and two pulses;
- modified trapezoid motion input, pre-shaping with one frequency and three pulses;
- modified trapezoid motion input, pre-shaping with two frequencies and three pulses.

All the simulations have been carried out for a rotation of 120° and compared with each other. The maximum angular velocity imposed at the revolute joint was of 0.8 rad/s and the maximum angular acceleration was of 0.4 rad/s^2.

Among the results obtained – such as the displacement at the end of the arm in an absolute reference system, the velocity and the acceleration at the free-end and at the revolute joint – only the comparison between the displacements at the end of the arm is reported in Figs. 7–14. The different figures, at the left

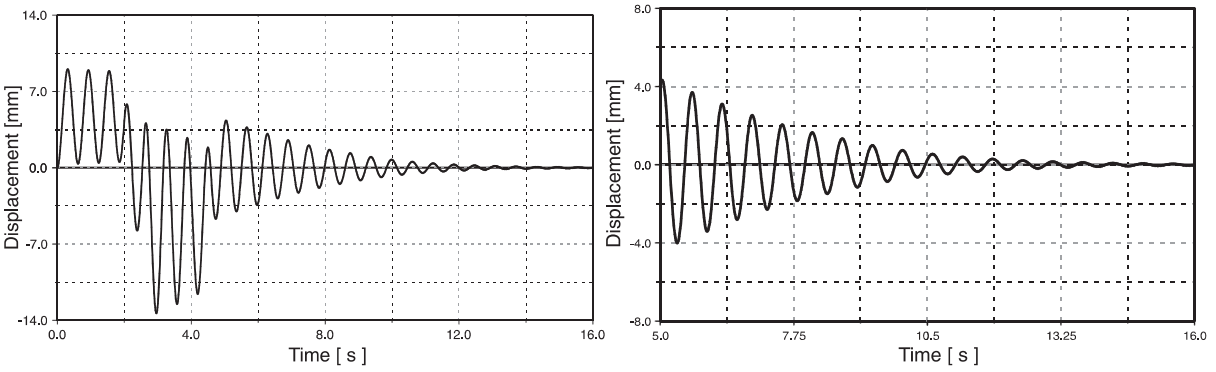

Fig. 7. Response to constant acceleration motion input (left), free motion after positioning (right).

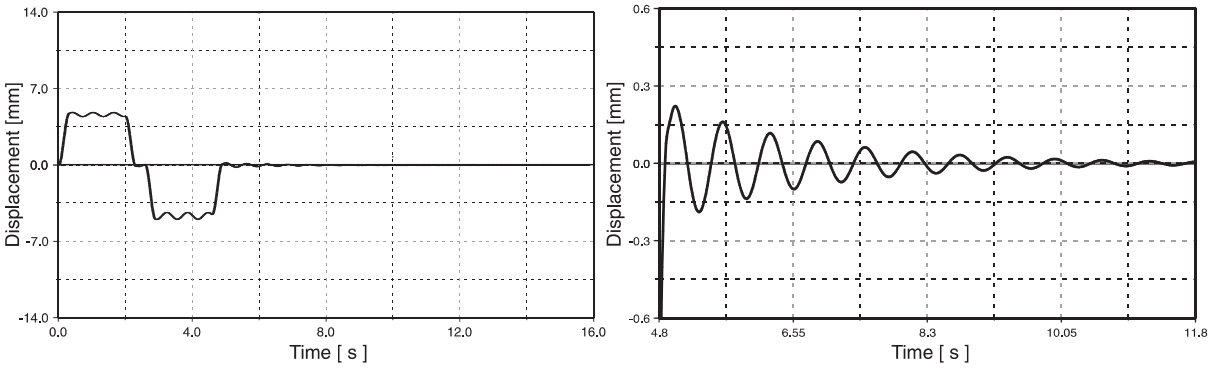

Fig. 8. Response to pre-shaped constant acceleration motion input with two pulses on first natural frequency (left), free motion after positioning (right).

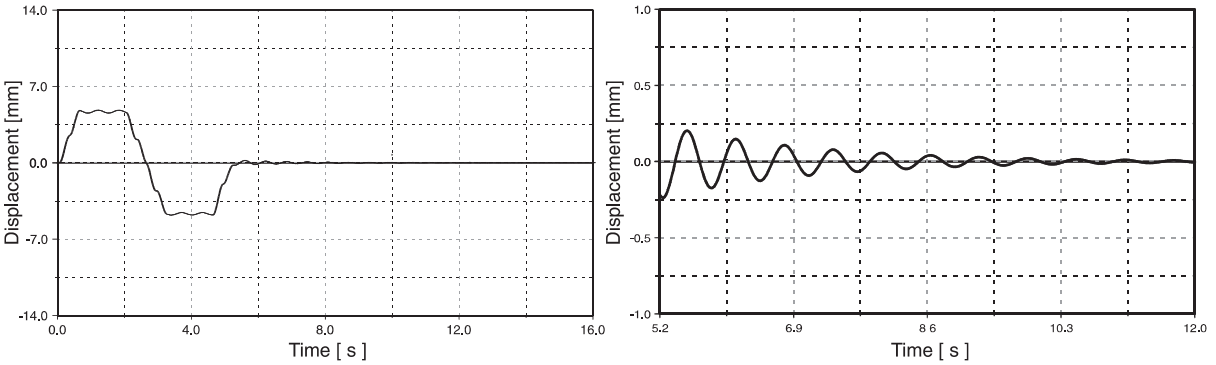

Fig. 9. Response to pre-shaped constant acceleration motion input with three pulses on first natural frequency (left), free motion after positioning (right).

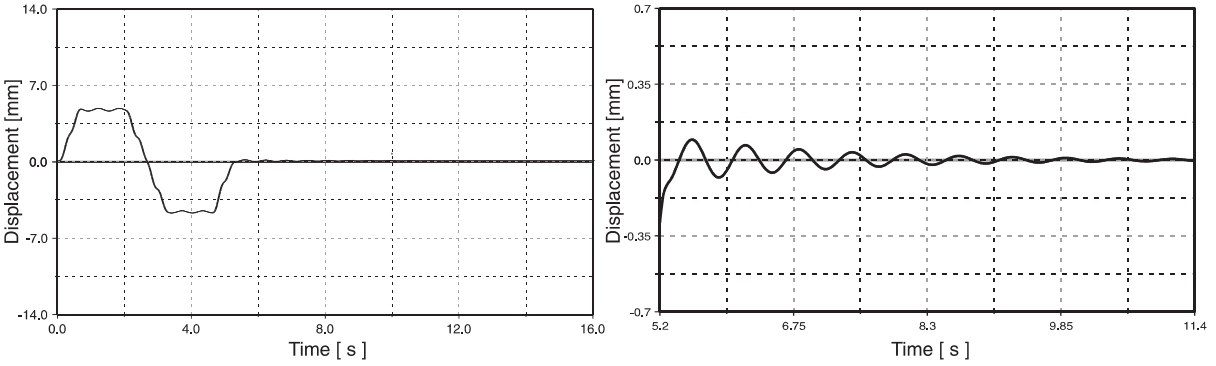

Fig. 10. Response to pre-shaped constant acceleration motion input with three pulses on first and second natural frequencies (left), free motion after positioning (right).

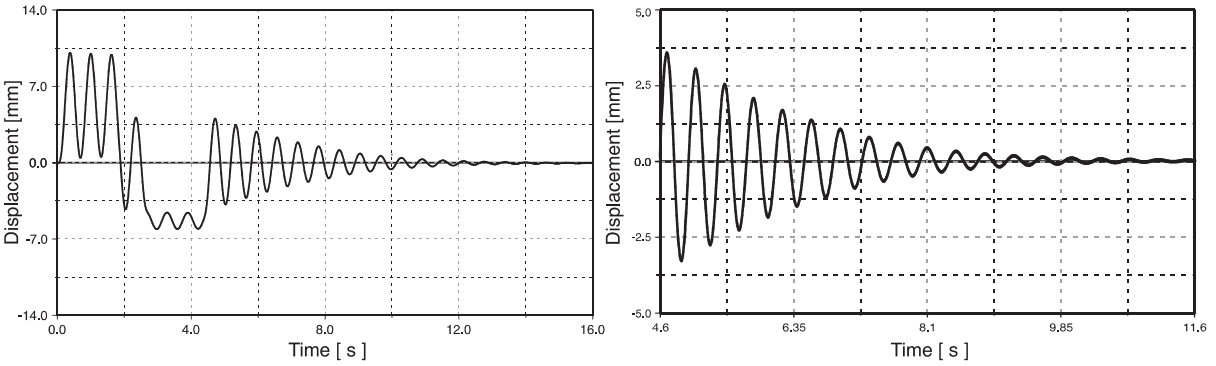

Fig. 11. Response to modified trapezoid motion input (left), free motion after positioning (right).

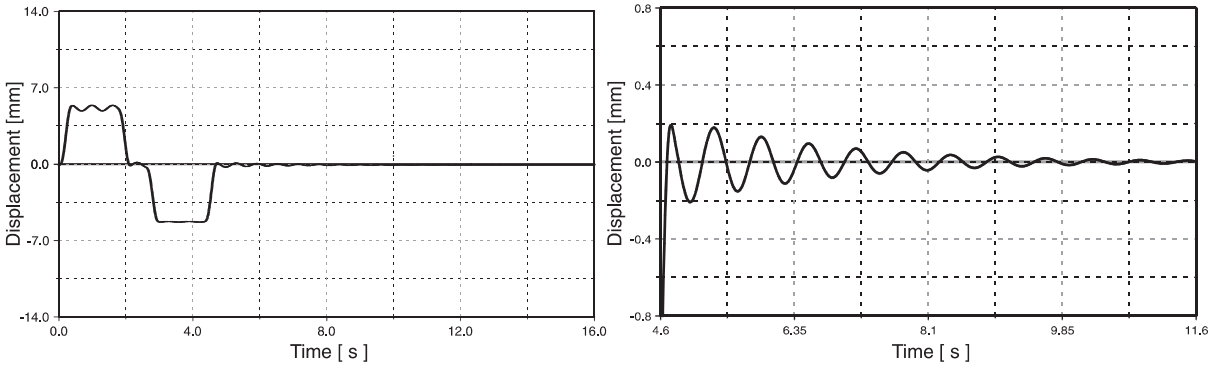

Fig. 12. Response to pre-shaped modified trapezoid motion input with two pulses on first natural frequency (left), free motion after positioning (right).

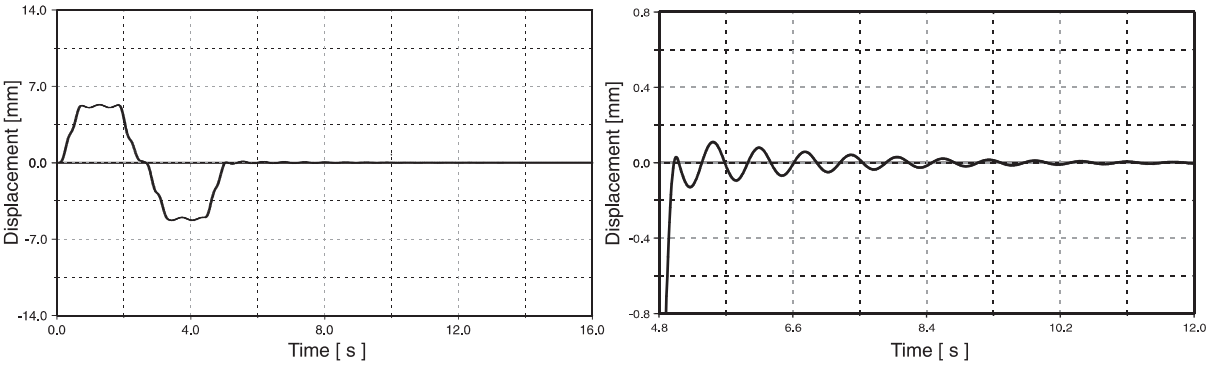

Fig. 13. Response to pre-shaped modified trapezoid motion input with three pulses on first natural frequency (left), free motion after positioning (right).

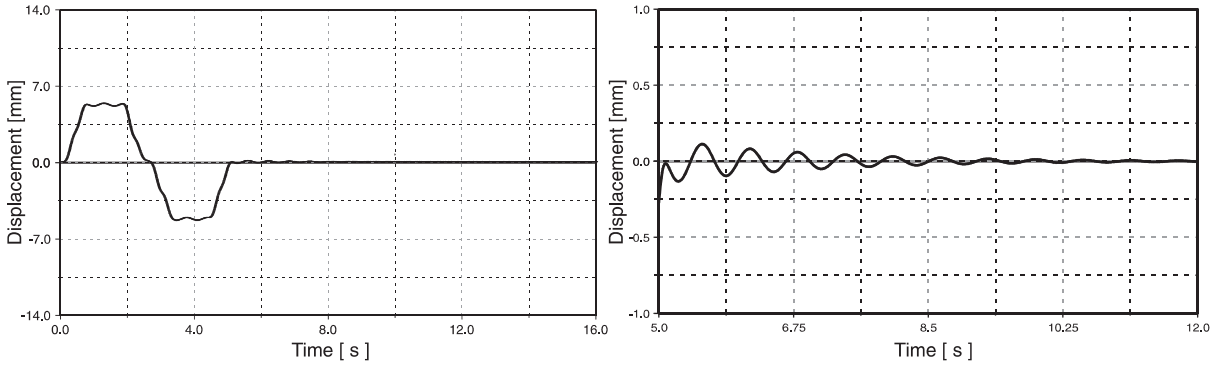

Fig. 14. Response to pre-shaped modified trapezoid motion input with three pulses on first and second natural frequencies (left), free motion after positioning (right).

side, are plotted in the same scale. For a better evaluation of the results, the displacement at the end of the positioning is reported separately on the right side. However, in this case, it would not be possible to use the same scale since the positioning takes slightly different times depending on the motion input, and the residual vibration has a wide range of variation.

Table 1 summarizes the results, by comparing the amplitude of the residual vibration after 6.5 s of simulation, calculated as the damped exponential envelope of the vibration. The comparison of the performances obtained by different motion inputs for the reduction of the residual vibration at the end of positioning has to be done on the basis of a given benchmark, which is the response of the system to the constant acceleration motion input, shown in Fig. 7. By first considering the comparison with the modified trapezoid motion input, it is possible to note a reduction of the vibration amplitude (Fig. 11). This is strictly correlated to the modification of the motion input, with respect to the constant acceleration input. In fact, the latter has impulsive variation of the acceleration that excites a wide range of frequencies and that is not tuned in order to delete the relative effect as it is done in the case of the pre-shaping. A more significant reduction is obtained with both the constant acceleration and the modified trapezoid pre-shaped inputs. In these cases, given the number of pulses and the frequencies considered, the different performances between the pre-shaped inputs obtained from the constant acceleration or the modified trapezoid are minimal.

Moreover, since only the first mode appears to be excited in the simulations, the results obtained with the use of the pre-shaping based on two frequencies do not show improvement with respect to the cases with just one frequency. However, it has been considered important to show the simulations also in this case, since when a more complicated structure is considered, e.g. with two links, the effect of considering also the second frequency is not negligible (Mimmi and Pennacchi, 2000).

Table 1
Comparison of the different motion inputs

Motion input	Amplitude after 6.5 s in mm
Constant acceleration motion input	3.75
Constant acceleration motion input, pre-shaping with one frequency and two pulses	0.14
Constant acceleration motion input, pre-shaping with one frequency and three pulses	0.13
Constant acceleration motion input, pre-shaping with two frequencies and three pulses	0.12
Modified trapezoid motion input	1.25
Modified trapezoid motion input, pre-shaping with one frequency and two pulses	0.1
Modified trapezoid motion input, pre-shaping with one frequency and three pulses	0.09
Modified trapezoid motion input, pre-shaping with two frequencies and three pulses	0.09

5. Conclusions

In this paper, we have presented the comparison between different motion inputs in order to reduce the residual vibration after positioning of a flexible manipulator arm. The model of the flexible arm has been implemented in a multibody program, and several simulations have been carried out. From the simulations, it is possible to stress the following:

- Motion inputs with pre-shaping are always better than original motion inputs. Therefore, it is useless to apply pre-shaping to complicated motion inputs: i.e. a motion input with pre-shaping obtained from constant acceleration gives better results than a plain modified trapezoid.
- Once the number of pulses and frequencies considered for the pre-shaping is given, the motion obtained by the modified trapezoid gives better performances than those by constant acceleration. The difference is very small, so the choice of applying such a complicated motion input has to be carefully considered.
- If the electric motor can follow complex motion inputs, the use of input with pre-shaping is convenient; otherwise, the use of a plain modified trapezoid motion input may reduce the residual vibration. In this case, the motion input can be further tuned by operating on the steps δ_i of the algorithm of the input generation.

Acknowledgements

This work has been funded, in part, by ASI Contract 2/296-Ricerca Fondamentale '97 provided by ASI (Agenzia Spaziale Italiana-Italian Space Agency).

Appendix A

A.1. Constant acceleration motion input

Given the maximum value available for the angular velocity $\dot{\varphi}_{\max}$, that of the maximum imposed angular acceleration $\ddot{\varphi}_{\max}$ and the required rotation $\bar{\varphi}$, it is possible to determine the time $\bar{t}$ needed for the operation. This can be done by means of the following algorithm:

(1) Let the time necessary for the rotation be supposed equal to $\bar{t}$. It is divided into three parts δ_1, δ_2 and δ_3 (Fig. 1) with the following constraint between the values of t_i and δ_i:

$$\sum_{i=1}^{3}\delta_i = \bar{t}, \qquad t_k = \sum_{i=1}^{k}\delta_i. \tag{A.1}$$

(2) At the end of the first step, δ_1, the maximum velocity will be reached $\dot{\varphi}_{\max}$; moreover, since the system has arrived at the instant t_1 with constant acceleration, it results that

$$\dot{\varphi}_1 = \dot{\varphi}_{\max} = \ddot{\varphi}_{\max}\delta_1 \rightarrow \delta_1 = \frac{\dot{\varphi}_{\max}}{\ddot{\varphi}_{\max}}. \tag{A.2}$$

(3) By considering that the system has to arrive at $\bar{\varphi}$ with null velocity at the final instant $\bar{t}$, it is possible to impose this constraint by evaluating the corresponding expression of φ_3 and $\dot{\varphi}_3$:

$$\begin{aligned} &\dot{\varphi}_3 = 0 = \dot{\varphi}_{\max} - \ddot{\varphi}_{\max}\delta_3, \\ &\varphi_3 = \bar{\varphi} = \dot{\varphi}_{\max}\delta_2 + \tfrac{1}{2}\ddot{\varphi}_{\max}\delta_1^2 + \dot{\varphi}_{\max}\delta_3 - \tfrac{1}{2}\ddot{\varphi}_{\max}\delta_3^2. \end{aligned} \tag{A.3}$$

(4) If we make a system with Eqs. (A.2) and (A.3), the duration of the intervals δ_i are determined, and thus also $\bar{t}$ with the first of Eq. (A.1):

$$\delta_1 = \frac{\dot{\varphi}_{\max}}{\ddot{\varphi}_{\max}}, \qquad \delta_2 = \frac{\bar{\varphi}\ddot{\varphi}_{\max} - \dot{\varphi}^2_{\max}}{\dot{\varphi}_{\max}\ddot{\varphi}_{\max}}, \qquad \delta_3 = \frac{\dot{\varphi}_{\max}}{\ddot{\varphi}_{\max}}. \tag{A.4}$$

For instance, the time histories of $\ddot{\varphi}, \dot{\varphi}, \varphi$ are shown in Fig. 1, as regards a rotation of 1.57 rad, where the maximum angular velocity and acceleration are, respectively, 0.5 rad/s and 1 rad/s^2.

A.2. Modified trapezoid motion input

Let the time necessary for the rotation equal to angle $\varphi_{\text{tot}} = \bar{\varphi}$ be supposed equal to $\bar{t}$. The algorithm follows these steps:

(1) The time interval $\bar{t}$ is divided into seven parts $\delta_1, \delta_2, \delta_3, \delta_4, \delta_5, \delta_6$ and δ_7, which can be equal to zero if that is the case (Fig. 15) with the following constraint between the values of t_i and δ_i:

$$\sum_{i=1}^{7}\delta_i = \bar{t}, \qquad t_k = \sum_{i=1}^{k}\delta_i. \tag{A.5}$$

(2) If sinusoid arcs connect the constant acceleration intervals, the inertia force variation is not impulsive. Therefore, if the initial conditions are $\varphi_0 = 0$ and $\dot{\varphi}_0 = 0$, the corresponding command input for angular acceleration and angular velocity are of the type reported in Fig. 15. The analytical expression of the different arcs is reported in Magnani and Ruggieri (1986);

(3) Now, the constraint on the maximum available motor velocity is introduced by observing that the maximum velocity $\dot{\varphi}_{\max}$, is reached at the end of interval δ_3, where the velocity value is

$$\dot{\varphi}_3 = \dot{\varphi}_2 + A\frac{2\delta_3}{\pi}. \tag{A.6}$$

For the determination of $\dot{\varphi}_3$, it is necessary to go back to the instant $t = 0$, by also determining the velocities $\dot{\varphi}_2$ and $\dot{\varphi}_1$ at the end of intervals δ_2 and δ_1:

$$\dot{\varphi}_2 = \dot{\varphi}_1 + A\delta_2, \qquad \dot{\varphi}_1 = A\frac{2\delta_1}{\pi}. \tag{A.7}$$

The constant A can be determined by imposing the rotation φ_7 equal to $\bar{\varphi}$ and the velocity $\dot{\varphi}_7$ of null value, i.e. the point-to-point operation is concluded with null final velocity:

$$\begin{cases} \varphi_7 = \bar{\varphi}, \\ \dot{\varphi}_7 = 0. \end{cases} \tag{A.8}$$

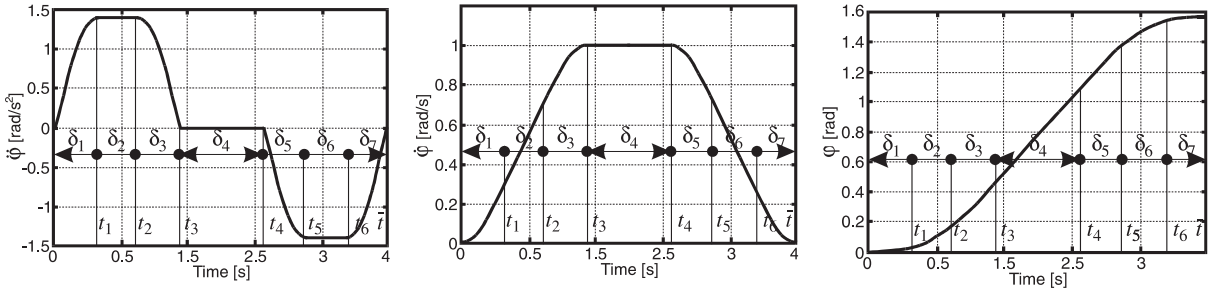

Fig. 15. Modified trapezoid motion input.

Eq. (A.8) leads to

$$A = \bar{\varphi}\left[\begin{array}{c|c} \dfrac{2\delta_5}{\pi}+\delta_6+\dfrac{2\delta_7}{\pi} & \\ \hline \dfrac{2\delta_1}{\pi}+\delta_2+\dfrac{2\delta_3}{\pi} & -\dfrac{2\delta_5}{\pi}-\delta_6-\dfrac{2\delta_7}{\pi} \\ \hline \dfrac{2\delta_1}{\pi}\left(\dfrac{\pi-2}{\pi}\delta_1+\dfrac{\delta_2}{2}\right)+\left(\dfrac{2\delta_1}{\pi}+\delta_2\right)\left(\dfrac{\delta_2}{2}+\dfrac{\pi-2}{\pi}\delta_3\right)+ & \left(\dfrac{2\delta_7}{\pi}+\delta_6\right)\left(\dfrac{\pi-2}{\pi}\delta_5+\dfrac{\delta_6}{2}\right)+\dfrac{2\delta_7}{\pi}\left(\dfrac{\delta_6}{2}+\dfrac{\pi-2}{\pi}\delta_7\right) \\ +\left(\dfrac{2\delta_1}{\pi}+\delta_2+\dfrac{2\delta_3}{\pi}\right)\left(\dfrac{2\delta_3}{\pi}+\delta_4+\dfrac{2\delta_5}{\pi}\right) & \end{array}\right] \tag{A.9}$$

Therefore, once given the δ_i sequence, the minimum time $\bar{t}$ satisfies the following equation:

$$\dot{\varphi}_3 = \dot{\varphi}_{\max} \rightarrow A(\bar{t})\left(\frac{2\delta_1(\bar{t})}{\pi}+\delta_2(\bar{t})+\frac{2\delta_3(\bar{t})}{\pi}\right) = \dot{\varphi}_{\max}. \tag{A.10}$$

(4) At this point, both the rotation $\bar{\varphi}$ and the actual time $\bar{t}$ for the operation are known and the algorithm loops back to point 1 to define the actual command inputs.

Note that the algorithm described presents an arbitrary choice for the intervals δ_i and that the calculation of the time $\bar{t}$ depends on this choice. In fact, the more the interval at $\dot{\varphi}_{\max}$ constant velocity is extended, the more the operation time is reduced.

A.3. Pre-shaping method

In this part of the appendix, the calculations for determining the pulse amplitude and their temporal sequence are reported. This allows the pre-shaping method to be applied to the motion input. The starting point is the response of a system to a general succession of n pulses. In particular the response to the pulse applied at time t_j is

$$y_j(t) = A_j\frac{\omega_0}{\sqrt{1-\xi^2}}e^{-\xi\omega_0(t-t_j)}\sin\left(\omega_0\sqrt{1-\xi^2}(t-t_j)\right). \tag{A.11}$$

By doing the following substitutions

$$B_j = \frac{A_j\omega_0}{\sqrt{1-\xi^2}}e^{-\xi\omega_0(t_f-t_j)}, \qquad \alpha = \omega_0\sqrt{1-\xi^2}, \qquad \phi_j = -\omega_0\sqrt{1-\xi^2}t_j \tag{A.12}$$

and using them in Eq. (A.11), the response to the jth pulse becomes

$$y_j(t) = B_j\sin(\alpha t+\phi_j). \tag{A.13}$$

If we consider a case with two pulses and the system is linear, the responses can be superimposed:

$$B_1\sin(\alpha t+\phi_1)+B_2\sin(\alpha t+\phi_2) = A_{\text{amp}}\sin(\alpha t+\psi), \tag{A.14}$$

where

$$\begin{aligned} A_{\text{amp}} &= \sqrt{(B_1\cos\phi_1+B_2\cos\phi_2)^2+(B_1\sin\phi_1+B_2\sin\phi_2)^2}, \\ \psi &= \tan^{-1}\left(\frac{B_1\cos\phi_1+B_2\cos\phi_2}{B_1\sin\phi_1+B_2\sin\phi_2}\right). \end{aligned} \tag{A.15}$$

The condition of having no residual vibration at the end of the pulse sequence is given by the null amplitude A^{amp}, which is equivalent to

$$\begin{cases} A_1 e^{-\xi\omega_0(t_f-t_1)} \sin\left(t_1\omega_0\sqrt{1-\xi^2}\right) + A_2 e^{-\xi\omega_0(t_f-t_2)} \sin\left(t_2\omega_0\sqrt{1-\xi^2}\right) = 0, \\ A_1 e^{-\xi\omega_0(t_f-t_1)} \cos\left(t_1\omega_0\sqrt{1-\xi^2}\right) + A_2 e^{-\xi\omega_0(t_f-t_2)} \cos\left(t_2\omega_0\sqrt{1-\xi^2}\right) = 0. \end{cases} \tag{A.16}$$

There are four unknowns in system (A.16), A_1, A_2, t_1 and t_2, with only two equations. Due to the arbitrariness in the application of the pulses, it is possible to apply the first at time $t_1 = 0$. A further condition can be obtained by the normalization of the pulse amplitude, whose sum has to be equal to the unitary pulse, in order to guarantee that the signal is not amplified. Therefore, the system becomes

$$\begin{cases} A_1 e^{-\xi\omega_0(t_f-t_1)} \sin\left(t_1\omega_0\sqrt{1-\xi^2}\right) + A_2 e^{-\xi\omega_0(t_f-t_2)} \sin\left(t_2\omega_0\sqrt{1-\xi^2}\right) = 0, \\ A_1 e^{-\xi\omega_0(t_f-t_1)} \cos\left(t_1\omega_0\sqrt{1-\xi^2}\right) + A_2 e^{-\xi\omega_0(t_f-t_2)} \cos\left(t_2\omega_0\sqrt{1-\xi^2}\right) = 0, \\ t_1 = 0, \\ A_1 + A_2 = 1. \end{cases} \tag{A.17}$$

From the first equation of system (A.17), it follows that

$$A_2 e^{-\xi\omega_0(t_f-t_2)} \sin\left(t_2\omega_0\sqrt{1-\xi^2}\right) = 0. \tag{A.18}$$

In order for Eq. (A.18) to be satisfied, by excluding the trivial solution $A_2 = 0$, the argument of sine function has to be null. This condition allows the value t_2 to be calculated:

$$t_2\omega_0\sqrt{1-\xi^2} = \pm n\pi \tag{A.19}$$

with $n \in \mathbb{N}$; since $t_2 > 0$, from Eq. (A.19), by considering the first time step acceptable, it follows that

$$t_2 = \frac{\pi}{\omega_0\sqrt{1-\xi^2}}. \tag{A.20}$$

By using Eq. (A.20) in the second equation of system (A.17) and with suitable transformations, we have

$$A_1 + A_2 e^{\xi\pi/\sqrt{1-\xi^2}} \cos\pi = 0 \rightarrow A_1 - A_2 e^{\xi\pi/\sqrt{1-\xi^2}} = 0, \tag{A.21}$$

and finally, by considering the third equation of system (A.17):

$$t_1 = 0, \qquad A_1 = \frac{1}{1+K}, \qquad t_2 = \Delta T, \qquad A_2 = \frac{K}{1+K} \quad \text{with } K = e^{-\xi\pi/\sqrt{1-\xi^2}}, \ \Delta T = \frac{\pi}{\omega\sqrt{1-\xi^2}}. \tag{A.22}$$

If three pulses are taken into account, two further unknowns have to be calculated: the time t_3 and the amplitude of the third pulse A_3. The new constraints can be obtained on the condition that also the derivative of Eqs. (A.16) have to be equal to zero. This is equivalent to considering that the system, at the end of the third pulse, has null amplitude and velocity of vibration. The remaining conditions of applying the first pulse at the initial time and the condition on the sum of the amplitudes are the same of the two pulse case, therefore the system becomes

$$\begin{cases} A_1 e^{-\xi\omega_0(t_f-t_1)} \sin\left(t_1\omega_0\sqrt{1-\xi^2}\right) + A_2 e^{-\xi\omega_0(t_f-t_2)} \sin\left(t_2\omega_0\sqrt{1-\xi^2}\right) + A_3 e^{-\xi\omega_0(t_f-t_3)} \sin\left(t_3\omega_0\sqrt{1-\xi^2}\right) = 0, \\ A_1 e^{-\xi\omega_0(t_f-t_1)} \cos\left(t_1\omega_0\sqrt{1-\xi^2}\right) + A_2 e^{-\xi\omega_0(t_f-t_2)} \cos\left(t_2\omega_0\sqrt{1-\xi^2}\right) + A_3 e^{-\xi\omega_0(t_f-t_3)} \cos\left(t_3\omega_0\sqrt{1-\xi^2}\right) = 0, \\ A_1 t_1 e^{-\xi\omega_0(t_f-t_1)} \sin\left(t_1\omega_0\sqrt{1-\xi^2}\right) + A_2 t_2 e^{-\xi\omega_0(t_f-t_2)} \sin\left(t_2\omega_0\sqrt{1-\xi^2}\right) + A_3 t_3 e^{-\xi\omega_0(t_f-t_3)} \sin\left(t_3\omega_0\sqrt{1-\xi^2}\right) = 0, \\ A_1 t_1 e^{-\xi\omega_0(t_f-t_1)} \cos\left(t_1\omega_0\sqrt{1-\xi^2}\right) + A_2 t_2 e^{-\xi\omega_0(t_f-t_2)} \cos\left(t_2\omega_0\sqrt{1-\xi^2}\right) + A_3 t_3 e^{-\xi\omega_0(t_f-t_3)} \cos\left(t_3\omega_0\sqrt{1-\xi^2}\right) = 0, \\ t_1 = 0, \\ A_1 + A_2 + A_3 = 1. \end{cases} \tag{A.23}$$

Similar to the case of two pulses from the first and the third equation of system (A.23), by considering the argument of sine functions as null, we have

$$t_2 = \frac{\pi}{\omega_0\sqrt{1-\xi^2}}, \qquad t_3 = \frac{2\pi}{\omega_0\sqrt{1-\xi^2}}. \tag{A.24}$$

By substituting the values of Eqs. (A.24) in the second and fourth equations of system (A.23) and by solving the latter with the sixth equation, we finally have

$$t_1 = 0, \qquad A_1 = \frac{1}{1+2K+K^2}, \qquad t_2 = \Delta T, \qquad A_2 = \frac{2K}{1+2K+K^2}, \qquad t_3 = 2\Delta T,$$
$$A_3 = \frac{K^2}{1+2K+K^2} \quad \text{with } K = e^{-\xi\pi/\sqrt{1-\xi^2}}, \quad \Delta T = \frac{\pi}{\omega\sqrt{1-\xi^2}}. \tag{A.25}$$

References

Bhat, S.P., Miu, D.K., 1990. Precise point to point positioning control of flexible structures. ASME Journal of Dynamic Systems, Measurement and Control 112 (4), 667–674.

Jayasuriya, S., Choura, S., 1991. On the finite settling time and residual vibration control of flexible structures. ASME Journal of Sound and Vibration 148 (1), 117–136.

Magnani, P.L., Ruggieri, G., 1986. Meccanismi per macchine automatiche. UTET, Torino, pp. 106–112.

Meckl, P., Seering, W., 1985a. Active damping in a three-axis robotic manipulator. ASME Journal of Vibration, Acoustics, Stress and Reliability in Design 107, 38–46.

Meckl, P., Seering, W., 1985b. Minimizing residual vibration for point-to-point motion. ASME Journal of Vibration, Acoustics, Stress and Reliability in Design 107, 378–382.

Mimmi, G., Pennacchi, P., Bernelli-Zazzera, F., 1999. Minimizing residual vibration for flexible manipulator in point to point operations. Proceedings of PACAM VI (Sixth Pan American Congress of Applied Mechanics)-DINAME '99, Rio de Janeiro, Brazil, January 4–8, 1999.

Mimmi, G., Pennacchi, P., 2000. Controllo in anello aperto di un manipolatore flessibile. Il Progettista Industriale, No.1, Gennaio.

Onsai, T., Akay, A., 1991. Vibration reduction of a flexible arm by time-optimal open-loop control. ASME Journal of Sound and Vibration 147 (2), 283–300.

Rao, S.S., 1995. Mechanical Vibrations. Addison-Wesley, Reading, MA, pp. 523–534.

Singer, N.C., Seering, W.P., 1990. Preshaping command inputs to reduce system vibration. ASME Journal of Dynamic Systems, Measurement and Control 112, 76–82.

Singh, T., Heppler, G.R., 1993. Shaped input control of a system with multiple modes. ASME Journal of Dynamic Systems, Measurement and Control 115, 341–347.

Smith, O.J.M., 1958. Feedback Control Systems. McGraw-Hill, New York, p. 338.

Thomson, W.T., 1993. Theory of Vibration with Applications. Chapman and Hall, London, pp. 281–286.